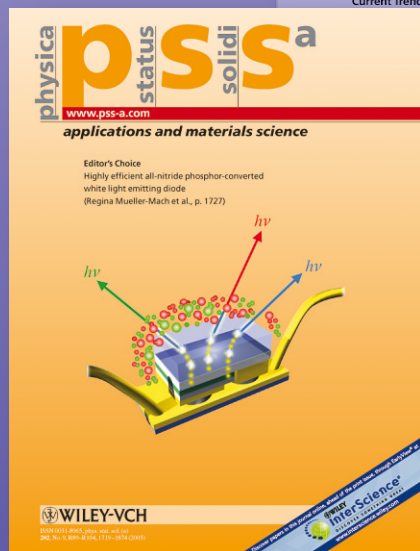


physica p status solidi S S

www.interscience.wiley.com

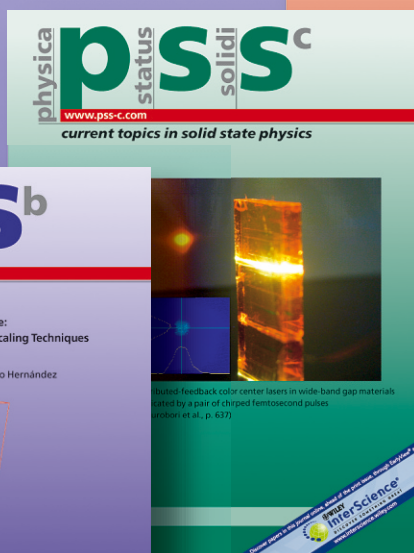
reprints



www.pss-a.com



www.pss-b.com



www.pss-c.com



www.pss-rrl.com

Fast macropore growth in n-type silicon

Ala Cojocaru*, Jürgen Carstensen, Emmanuel K. Ossei-Wusu, Malte Leisner, Oliver Riemenschneider, and Helmut Föll

Institute for Materials Science, Christian-Albrechts-University of Kiel, Kaiserstr. 2, 24143 Kiel, Germany

Received 7 March 2008, revised 29 October 2008, accepted 17 November 2008

Published online 5 February 2009

PACS 81.05.Rm, 82.45.Vp, 82.47.Wx, 84.37.+q

* Corresponding author: e-mail ac@tf.uni-kiel.de, Phone: +49 431 880 6180, Fax: +49 431 880 6178

Deep macropores can be grown in classical aqueous HF electrolytes only at slow etching speeds, fast macropores can only be grown to modest depths (150 μm). The addition of acid acetic to the electrolyte can roughly double the etching speed of the macropores, enabling quick and easy etching of pore depths as deep as 520 μm , and potentially more, if wafers thicker than 550 μm would be used. The addition of car-

boxymethylcellulose sodium salt (CMC) to the electrolyte decreases the roughness of the pore walls significantly. It is successfully shown that electrolytes consisting of HF + acetic acid + CMC can be utilized to produce fast, deep, and smooth macropores simultaneously in n-type silicon, required for a multitude of potential applications.

© 2009 WILEY-VCH Verlag GmbH & Co. KGaA, Weinheim

1 Introduction Since the discovery of macroporous silicon much progress was made towards the development of production technologies [1] and many product prototypes have been advanced (see e.g. [2] and references therein). A review concerning pores in Si and their intended applications, for example in micro electronic and mechanical systems, as x-ray filters, electrodes for micro fuel cells, sensors of all kinds, and optical applications can be found in [3]. Silicon macropores are the pores mostly considered for these novel products. Macroporous Si can be fabricated with straight pores and smooth pore walls by using back side illumination in n-type Si [1]. Nevertheless, despite all of this progress, no product based on porous Si can be found on the market at present. One of the reasons for this is the slow growth speed of the macropores, which is not conducive for effective mass production, since the market requires not only good quality pores but also short processing times. In this work, HF based electrolytes containing other components are used to etch macropores considerably faster, the quality and speed of growth of these pores will be discussed in the following parts of the manuscript.

2 Experimental results (100) oriented n-type Si wafers with low doping levels corresponding to a resistivity

of 20 Ωcm are used for etching macropores. An n^+ layer is present on the back side of the wafer for good ohmic contact to the sample. The etching is done using back side illumination (BSI) [4, 1] at 20 °C. The samples were pre-structured by standard photolithography (hexagonal lattice) before etching. Three different electrolytes have been used in this work and the respective results will be analyzed in a comparative study in this work: a) a classical electrolyte, 5 wt.% HF aq., b) an aqueous electrolyte with 10 wt.% HF and an additional amount of 30% acetic acid, and c) an aqueous-viscous electrolyte with 10 wt.% HF + 6.67 g/l of carboxymethylcellulose sodium salt (CMC) and 30% acetic acid. Both (classical) voltage and new illumination impedance spectroscopy have been performed in-situ during the pore etching with a dedicated system produced by ET&TE GmbH.

Using classical aqueous electrolytes at low concentrations, it is not difficult to etch macropores into n-type Si as deep as the typical wafer thickness (450–550 μm). In Fig. 1 this is shown for the standard 5 wt.% HF aqueous electrolyte (white circles). For 400 μm deep pores these conditions yield an average pore growth speed of 0.7 $\mu\text{m}/\text{min}$. An increase in the HF concentration to 10 wt.% or 15 wt.% will result in the desired increase of pore growth speed, but also in a big disadvantage. Pores cannot

be grown deeper than 150 μm due to the formation of a cavity, which is caused by a mass transfer insufficiency of chemical species which determine the oxide dissolution rate to the pore tips. The addition of CMC, and thus increasing the electrolyte's viscosity, basically yields the same pore depth as a function of etching time (not shown in Fig. 1) as in the case of pure aqueous electrolytes. A full treatise of this topic can be found in a second abstract [5] for the PSST 2008 conference.

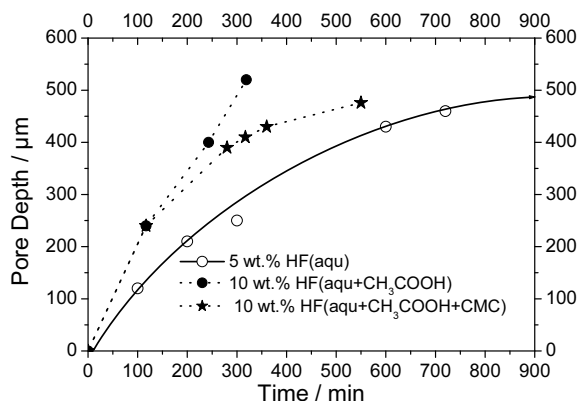


Figure 1 Pore depth vs. time for different HF based electrolytes: a) 5 wt.% HF aqueous (white circles), b) 10 wt.% HF + 30 wt.% CH_3COOH (black circles), c) 10 wt.% HF + 30 wt.% CH_3COOH + 6.67 g/l of carboxymethylcellulose sodium salt (black stars).

With the analyzed electrolytes containing acetic acid it was possible to increase the HF concentration, and thus the etching speed accordingly, to average etching speeds (for 400 μm pores) of 1.6 $\mu\text{m}/\text{min}$ and 1.4 $\mu\text{m}/\text{min}$ for the aqueous + acetic acid and the viscous + acetic acid electrolytes respectively. In Fig. 1 experiments with these electrolytes are illustrated by black circles and black stars, respectively. The aforementioned problem of cavity formation has not been observed during experiments with these electrolytes. Pore depths up to 520 μm could easily be achieved in short etching time, especially for the aqueous + acetic acid electrolyte. The results strongly indicate that even deeper macropores could be etched, if the wafer thickness (550 μm) would not be the limiting factor. It would be mentioned that addition of acetic acid to the electrolyte is not a general panacea, but must be turned to the HF concentration.

Most of the optical applications demand deep pores with very precise structural features: a constant diameter from top to tip, minimal roughness, etc. In [6] it was reported that viscous electrolytes increase the quality of the pore walls with regard to the pore wall roughness. Using the aqua-viscous electrolyte in combination with acetic acid, the quality of the pores increased substantially (see Fig. 2). Figure 2a represents the case of very deep pores etched with 10 wt.% HF + 30 wt.% acetic acid. As it can be seen, the pore walls are not very smooth (and some of the pores may stop to grow). In Fig. 2b the resulting pores

for the case of the aqua-viscous electrolyte + acetic acid are shown. Using this electrolyte, the quality of the pores was greatly increased and they grow to the same depth with smooth pore walls. Due to the viscosity, the pore growth speed decreased for deeper pores (more than 100 μm), as compared to the case without CMC, but it is still considerably larger than in the case of the 5 wt.% HF aq. electrolyte (Fig. 1). In total, 470 μm deep pores with a 1.5 $\mu\text{m}/\text{min}$ average growth rate could be obtained in the case of the aqua-viscous electrolyte.

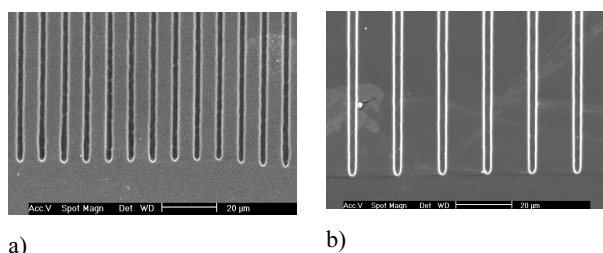


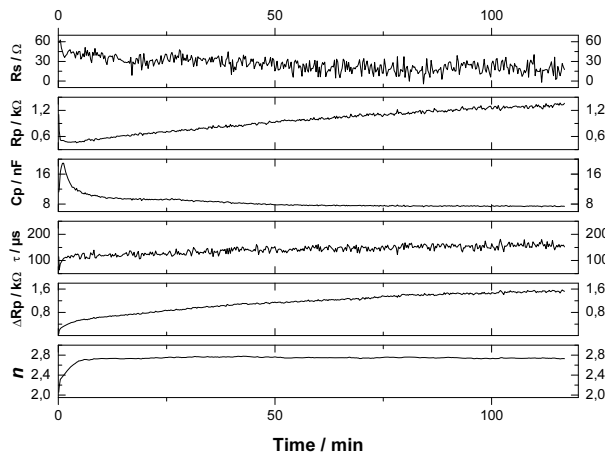
Figure 2 Deep and “fast” macropores etched in: a) aqueous electrolyte: 10 wt.% HF + 30 wt.% CH_3COOH and b) viscous-aqueous electrolyte: 10 wt.% HF + 30 wt.% CH_3COOH + 6.67 g/l CMC.

In-situ classical voltage and new illumination FFT impedance spectroscopy measurements have been performed. The measured data is fitted and interpreted by a model described in full detail in [7]. In Fig. 3 the model parameters are plotted as a function of the etching time. In the context of the model, in case of voltage impedance (Fig. 3a): R_S represents serial resistance accounting for the voltage losses at the contacts and electrolyte; R_P the chemical transfer resistance; τ time constant for the oxide dissolution– slow processes; The time constant τ describing the slow processes (according to the model the tetravalent dissolution), shows an increase in the beginning of the experiment, due to the reduction of the HF concentration at the pore tips, which is induced by the diffusion limitation. Later it becomes constant until the end of the experiment, reaching a steady state pore growth. This is an indication that the correlation between fast and slow is now in the optimum state for pore growth. ΔR_P represents the chemical transfer resistance of the slower partial dissolution reactions, e.g. mainly the indirect dissolution of Si.

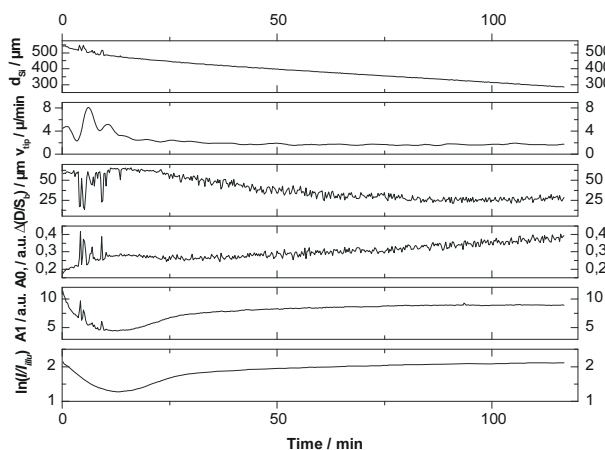
For illumination impedance (Fig. 3b): d_{Si} represents the thickness of the remaining bulk Si wafer, the negative derivative of this curve describes the velocity v_{tip} of pore growth at the tips; The velocity v_{tip} of pore growth at the tips (Fig. 3b) is constant for longer etching times and only in the beginning, when nucleation takes place, shows an increase and decay. The pore growth velocity is around 2 $\mu\text{m}/\text{min}$.

$\Delta(D/S_b)$ is the variation of the surface recombination velocity due to pore formation; A_0 describes the pore geometry; A_1 the over all etching area. The ratio between

etching current I and illumination intensity I_{illu} should increase monotonically and linearly with $\ln(I/I_{illu})$, which can be observed after the nucleation phase. This effect just reflects the additional increase in the area.



a)



b)

Figure 3 Time dependence of the impedance parameters (a) voltage impedance; (b) illumination impedance. Etching condition: 10 wt.% HF with 6.67 g CMC and 30 % acetic acid ($T = 20\text{ }^{\circ}\text{C}$, $U = 0.7\text{ V}$).

As can be seen from Fig. 3, all impedance fitting parameters show constant or just slight monotonic changes during the etching; only during the nucleation phase some deviations are observed.

3 Discussion As was presented in [5] the biggest problem for fast pore growth is the mass transfer diffusion limitation and too high applied etching currents, which require a high photocurrent and result in the cavity formation. The total flowing current through the pore is the sum of:

$$I_{total} = I_{tip} + I_{wall} + I_{photo}, \quad (1)$$

where I_{tip} – the leakage current flowing at the pore tip, I_{wall} – the leakage current flowing at pore wall and I_{photo} – photo-generated current at the pore tip. The leakage current is the amount:

$$I_{leak} = I_{tip} + I_{wall}. \quad (2)$$

A good interface passivation, i.e. lowest leakage current, will lead to increasing pore quality, and increasing speed of pore growth.

For a better interpretation of the obtained experimental data we assumed the existence of a critical current $I_{Crit}(d_{pore})$ as an upper limit for I_{total} . As long as I_{total} is lower than this critical current, the pore can grow. In terms of leakage current and photo current this means that for high photocurrent, as needed in the case of high HF concentration, which ensures a high speed of pore growth, the leakage current has to be as low as possible. As can be seen in Fig. 1a, using the acetic acid permits to obtain fast and very deep pores. This implies that the acetic acid drastically reduced I_{leak} by increasing the passivation of the pore walls.

In the case of lower HF concentration, resulting in lower I_{photo} , deep pores can be etched but need a lot of optimization, e.g. for the applied anodization voltage, temperature, etc., in the aim to decrease I_{leak} . As it was reported in [5], very deep pores could be obtained without optimization of the etching parameters. The viscosity reduced I_{leak} . Using the viscous electrolyte in combination with acetic acid for high HF concentration (Fig. 1b), fast, deep, and smooth pores could be obtained, implying that viscous electrolytes also lower I_{leak} .

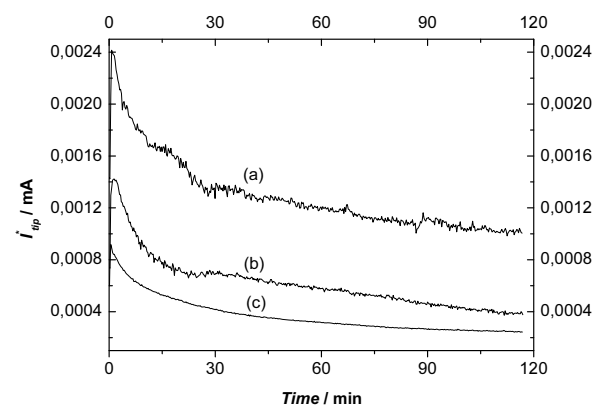


Figure 4 The leakage current I_{tip}^* according to Eq. (3): a) 1.0 V- applied voltage, 10 wt.% HF aqueous; b) 0.4 V- applied voltage, 10 wt.% HF aqueous; c) 0.7 V- applied voltage, 10 wt.% HF + 30 wt.% CH_3COOH .

From the impedance data the quantity I_{tip}^* can be derived:

$$I_{tip}^* = \frac{U}{R_s + R_p}, \quad (3)$$

which relates directly to the leakage current I_{tip} , as defined above. I_{tip}^* decreases with time, since the total current decreases. The interesting part is the relation of I_{tip}^* for various electrolytes. Plotting I_{tip}^* as shown in Fig. 4, a strong voltage dependence in the case of the classical aqueous electrolyte and significantly smaller currents for the acetic acid containing electrolyte are observed. For an applied voltage of 1.0 V (Fig. 4, curve a)) the I_{tip}^* is higher than in the case of 0.4 V (Fig. 4, curve b)), which is respectively higher than in the case of the acetic acid containing electrolyte for an applied voltage of 0.7 V (Fig. 4, curve c)). It is a good indication that in the case of the acetic acid electrolyte the leakage current strongly decreased.

4 Conclusion The addition of 30 % acetic acid allows for roughly double the etching speed of the macropores, enabling quick and easy etching of very deep pores. The uniformity of pore walls can be increased by viscous electrolytes.

All experimental results can be understood within a framework of diffusion limited pore growth and a strong dependence of the diffusion limitation to the leakage current mainly through pore walls.

A systematic search for other electrolytes which lead to a good interface passivation (i.e. small leakage currents) may even lead to further improvements with respect to pore growth speed and pore depth.

Acknowledgements Parts of this work have been supported by the Alexander von Humboldt foundation.

References

- [1] V. Lehmann, *Electrochemistry of Silicon* (Wiley-VCH, Weinheim, 2002).
- [2] L. T. Canham, A. Nassiopoulou, and V. Parkhutik (Eds.), *Phys. Status Solidi A* **202**(8), (2005).
- [3] H. Föll, M. Christophersen, J. Carstensen, and G. Hasse, *Mat. Sci. Eng. R* **39**(4), 93 (2002).
- [4] V. Lehmann and H. Föll, *J. Electrochem. Soc.* **137**(2), 653 (1990).
- [5] A. Cojocaru, J. Carstensen, M. Leisner, H. Föll, and I. M. Tiginyanu, *PSST 2008* (this conference).
- [6] E. Foca, J. Carstensen, M. Leisner, E. Ossei-Wusu, O. Riemenschneider, and H. Föll, *ECS Trans.* **6**(2), 367 (2007).
- [7] J. Carstensen, E. Foca, S. Keipert, H. Föll, M. Leisner, and A. Cojocaru, *Phys. Status Solidi A* **205**(11), 2485 (2008).